

JFM being a people-oriented programme, should have taken the people's confidence into account prior to initiating the village forest committees. However, in view of the target-oriented programme, the JFM was initiated primarily through enthusiasm of the Forest Department. The present study indicates that many species that are useful for the community have been cut due to removal of physical protection owing to the fact that these resources were not allowed to a part with the community. The community did not use the exotic species that were planted, and on the other hand, native species were used to meet their various biomass needs. The programme should develop measures that build up confidence in the village community before the formation of the forest committee. The social fencing attitude should be developed for their own benefit.

ests of Biligiri Rangan Hills, India. 2. Impact of NTFP extraction on regeneration, population structure and species composition. *Econ. Bot.*, 1996, **50**, 252–269.

19. Uma Shankar, Murali, K. S., Uma Shaanker, R., Ganeshaiah, K. N. and Bawa, K. S., Extraction of non-timber forest products in the forests of Biligiri Rangan Hills, India. 4. Impact of floristic diversity and population structure in a thorn scrub forest. *Econ. Bot.*, 1998, **52**, 302–315.

ACKNOWLEDGEMENTS. We thank Ford Foundation for supporting Ecology and Economics Research Network and Ministry of Environment and Forests, Govt. of India for support to CES, IISc, Bangalore. We thank Shri Deepak Shetty, C. M. Shastri, Gopal Hegde and Rozario Furtado at CES field station, Sirsi for help.

Received 26 April 2004; revised accepted 11 October 2004

1. Lal, J. B., Deforestation: causes and control. *Indian For.*, 1990, **116**, 431–441.
2. Shah, S. A., Ecological aspects of Indian forest management, In *New Voices in Indian Forestry* (ed. Kurup, V. S. P.), SPWD, New Delhi, 1996, pp. 49–82.
3. Myers, N., Tropical forests: The main deforestation fronts. *Environ. Conserv.*, 1993, **20**, 9–16.
4. Sandler, T., Tropical deforestation: Markets and market failures. *Am. J. Agric. Econ.*, 1993, **69**, 229–233.
5. Southgate, D., Sanders, J. and Ehui, S., Resource degradation in Africa and Latin America: Population pressure, policies and property arrangements. *Am. J. Agric. Econ.*, 1993, **72**, 1250–1263.
6. Ravindranath, N. H. and Hall, D. O., In *Biomass, Energy and Environment: A Developing Country Perspective from India*, Oxford University Press, New Delhi, 1995.
7. Murali, K. S. and Hegde, R., Patterns of tropical deforestation. *J. Trop. For. Sci.*, 1997, **9**, 465–476.
8. Saxena, N. C., The saga of participatory forest management in India. CIFOR special publication, Indonesia, 1997.
9. Bhat, D. M., Murali, K. S. and Ravindranath, N. H., Formation of secondary forests in southern India. *J. Trop. For. Sci.*, 2001, **13**, 601–620.
10. Saigal, S., Joint forest management: A decade and beyond. *INFORM*, 2001, **1**, 10–12.
11. Murali, K. S., Rao, R. J. and Ravindranath, N. H., Evaluation of JFM in India: A review of analytical processes. *Int. J. Environ. Sustainable Dev.*, 2002, **1**, 184–199.
12. Murthy, I. K., Murali, K. S., Hegde, G. T., Bhat, P. R. and Ravindranath, N. H., A comparative analysis of regeneration in natural forests and joint forest management plantations in Uttara Kannada district, Western Ghats. *Curr. Sci.*, 2002, **83**, 1358–1364.
13. Murali, K. S., Rao, R. J. and Ravindranath, N. H., Institutional and policy issues of participatory forestry: Indian experience. *Trop. Ecol.*, 2003, **44**, 73–84.
14. Bhat, P. R., Rao, R. J., Murthy, I. K., Murali, K. S. and Ravindranath, N. H., In *Joint Forest Planning and Management: A Micro and Macro Level Assessment* (eds Ravindranath, N. H., Murali, K. S. and Malhotra, K. C.), Oxford and IBH, New Delhi, 2000, pp 59–98.
15. Gaonkar, D. S. and Gowda, S. B., Joint forest planing and management in Uttara Kannada District, Karnataka. *Indian For.*, 2000, **126**, 554–568.
16. Magurran, A. E., In *Ecological Diversity and its Measurement*, Croom Helm Publishers, London, 1988.
17. Zar, H., In *Biostatistical Analysis*, Prentice Hall, New York, 1985.
18. Murali, K. S., Uma Shankar, Uma Shaanker, R., Ganeshaiah, K. N. and Bawa, K. S., Extraction of non-timber forest products in the for-

## Mesoscopic ductile shear zones from the Main Central Thrust zone of Bhagirathi Valley, Garhwal Higher Himalaya

Nihar R. Tripathy and H. B. Srivastava\*

Department of Geology, Banaras Hindu University, Varanasi 221 005, India

**Mesoscopic ductile shear zones are well developed in the crystalline rocks of the Main Central Thrust (MCT) zone of Bhagirathi valley. Ductile and brittle-ductile shear zones are dominantly observed and exhibit both sinistral and dextral sense of sear. Detailed analysis reveals that NE-striking sinistral and NW-striking dextral shear zones form a conjugate pair. The bisectors of preferred orientations of these two sets of shear zones indicate that they developed in response to NNE–SSW horizontal compression synchronous to the translation of the MCT, which took place during the northward movement of the Indian Plate. Strain analysis reveals that the mesoscopic ductile shear zones developed in response to very high strain, in a narrow zone, which even deformed the internal fabrics of the rocks. The study of quartz *c*-axis fabrics in mesoscopic shear zones demonstrates that a single girdle pattern of quartz developed at the shear zone boundary and became prominent in the centre of the shear zone with increase in shear strain.**

DUCTILE shear zones are common features in crystalline rocks that have undergone natural deformation at moderate to high temperature<sup>1,2</sup>. They vary in width from millimetre to kilometre and displacements along them may vary from the same order of dimension as the width to several orders of magnitude larger<sup>3–6</sup>. In sections perpendicular to the plane of shear and parallel to the shear direction, they typically display a

\*For correspondence. (e-mail: harivandana@sify.com)



foliation with sigmoidal trace across the zone that increases in intensity from the edges towards the centre. The increase in foliation intensity can be related to an increase in strain and commonly also to a better-developed crystallographic fabric<sup>7-9</sup>. The analyses of shear zones provide many useful parameters such as shear strain, amount and direction of tectonic transport, percentage of volume loss<sup>6</sup>, and compression direction<sup>10</sup>.

In this communication we have examined several mesoscopic shear zones developed in the crystalline rocks of the Main Central Thrust (MCT) zone along Bhagirathi Valley, Garhwal Himalaya (Figure 1). Analysis of these shear zones enables us to determine the compressive stress directions acted during the development of these shear zones and places a reasonable constraint on the large-scale shear displacement.

In the Bhagirathi Valley, Garhwal Himalaya (Figure 1), the MCT forms a 10–12 km thick NNE-dipping shear zone<sup>11</sup>. The lower boundary of this shear zone corresponds to the Munsiri Thrust<sup>12</sup>. However, this thrust was first defined as the MCT<sup>13</sup> in the Alaknanda Valley. In the Bhagirathi Valley (Figure 1), the northerly dipping Munsiri Thrust or MCT separates the crystalline rocks of the Munsiri Group from the quartzites and metavolcanics of the Garhwal Group<sup>14</sup>. Further north, the rocks of the Munsiri Group are separated from the rocks of the Vaikrita Group of the Higher Himalaya along Vaikrita Thrust (Figure 1). Thus, the Munsiri Thrust marks the MCT zone in the south and the Vaikrita Thrust in the north. Augen gneisses, calcic migmatite schists, amphibolites and migmatite gneisses constitute the main lithological units of the MCT zone (Figure 2). The rocks of the MCT zone exhibit a dip of about 40–45° in NNE direction. Above the Munsiri Thrust, the metamorphic grade increases upwards the structural section.

Bedding plane (S1), though rarely seen, exhibits isoclinal folding in the quartzo-feldspathic layers in the gneisses of the area. In the MCT zone, foliation (S2) is defined by parallel arrangements of platy and flaky minerals exhibiting variation in strike from NNW to WNW, mainly dipping towards the northern direction. The linear fabrics developed in the MCT

zone are dominantly stretching lineations that trend in N to NNE direction with low to moderate amount of plunge. Adjacent to the Munsiri Thrust, stretching lineations are oriented parallel to the strike<sup>15</sup>. The foliations have an anastomosing geometry/pattern similar to the S–C fabric<sup>16</sup>. The schists and gneisses exhibit several mesoscopic ductile shear zones (Figure 3), and discrete zones, where the S–C fabric is developed. The geometry of the feldspar porphyroclasts and the S–C fabrics indicates evidence of top to SSW sense of shear<sup>11</sup>.

A ductile shear zone is a long, narrow zone within which dominantly ductile deformation has caused localization of large strain. The formation of a ductile shear zone is commonly associated with considerable reduction of grain size and development of a well-banded and lineated rock. In ductile shear zones, the differential displacements of the walls are accomplished entirely by the ductile flow and on outcrop scale it may not exhibit sharp discontinuities. Veins crossing the shear zones can be traced continuously through the zone, though they may be thinned (Figure 3b) where tangential displacement is large in comparison to the width of the shear zones<sup>17</sup>. At places where the veins are not present, the pre-shear foliation planes are sigmoidally curved (Figure 3c and d) in the shear zones and this helps to determine the sense of shear in the rocks<sup>8</sup>. Shear zones in which tangential (wall parallel) displacement takes place along brittle fractures (faults) and the wall rocks remain unstrained, are termed as brittle shear zones. Brittle–ductile shear zones are ductile shear zones with fault-like features at the centre of the shear zone against which marker layers are displaced abruptly. Ductile and brittle shear zones are, therefore, end-members in a continuous spectrum with brittle–ductile shear zones as intermediate types.

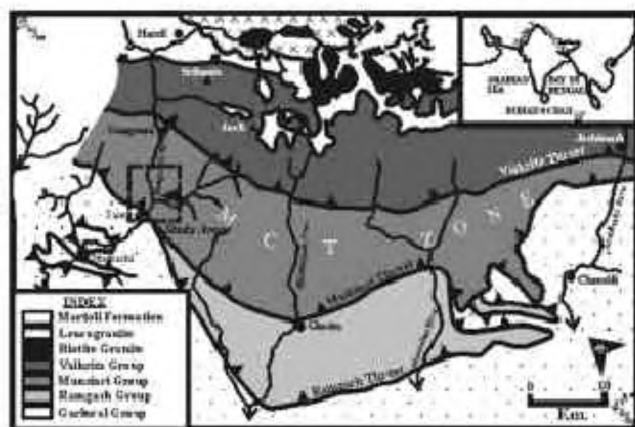


**Figure 1.** Tectonic map of Garhwal Himalaya (modified after Metcalfe<sup>11</sup>).

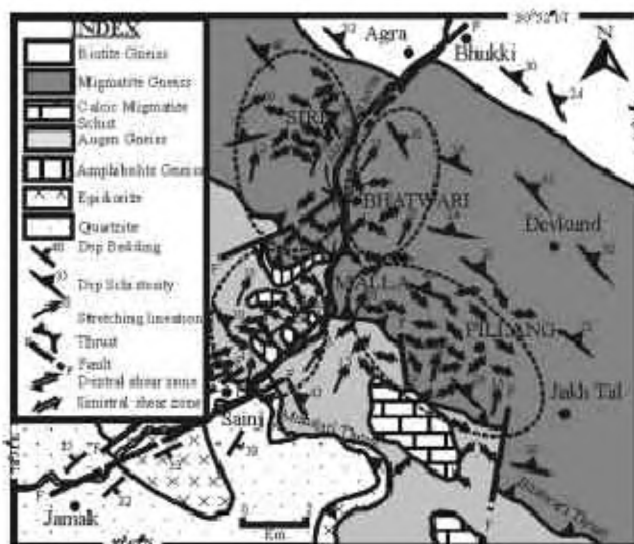


**Figure 2.** Geological map of the area around Bhatwari along Bhagirathi Valley. Elliptical broken lines are different sub-areas used for estimation of compressional direction. Data shown in different sub-areas are few representative ones; actual number of data for each sub-area is indicated in Figure 5.



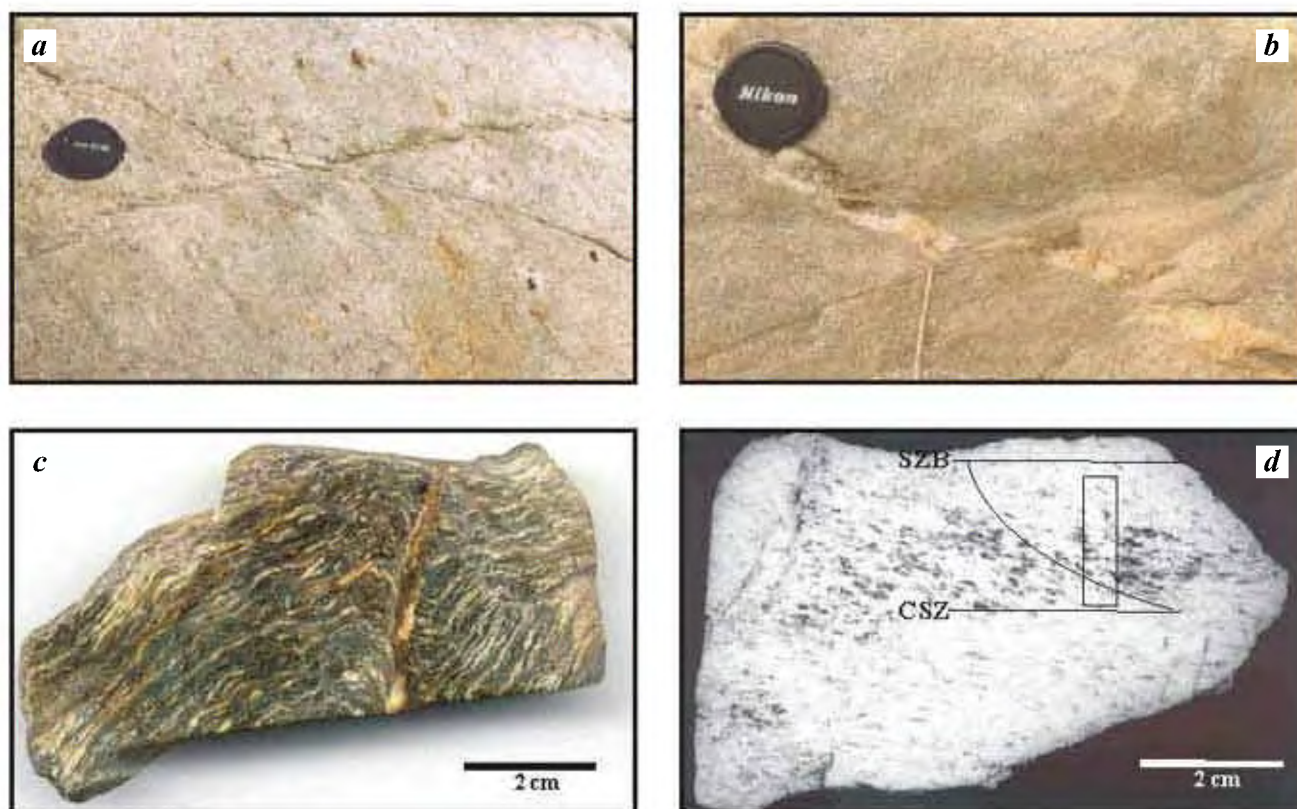


**Figure 3.** *a, b*, Field photograph of a conjugate ductile shear zone near Bhatwari. (*a*), and ductile shear zone exposed near Pillang gad (*b*). and *c, d*, Photograph of hand specimens of amphibolite gneisses showing sigmoidal pattern of schistosity (*c*) and hand specimen cut parallel to the *XZ* plane, exhibiting sigmoidal pattern of foliation, marked by dark biotite flakes. The rectangle marked has been used for strain and quartz *c*-axis analysis. SZB, Shear zone boundary; CSZ, Centre of shear zone.

All the three basic types of shear zones, viz. brittle, brittle-ductile, and ductile shear zones<sup>10</sup> are present in the area under study. However, ductile and brittle-ductile shear zones are much more common than the brittle shear zones. The strike length of these shear zones varies from 4 cm to 400 m, whereas the width varies from 3 mm to 100 m. These shear zones die out within few metres and exhibit moderate to steep dip. Near the terminations, ductile shear zones may widen with concomitant decrease in strain<sup>17</sup>. On shear surfaces, chlorite and biotite grains usually define a mineral lineation. Slickenside lineations have also been noted on brittle ductile and brittle shear zones. Both sinistral and dextral shear zones are present and they offset each other. A set of shear zones with the same sense of movement commonly remain parallel to each other over a considerable distance. Dextral and sinistral shear zones cross cut each other and enclose rhomb-shaped (Figure 3 *a*) areas.

Increase in the angle between shear zone walls and foliation trace indicates decrease in strain<sup>9</sup>. The sigmoidal foliation pattern, marked by biotite flakes in the gneisses (Figure 3 *d*), has been used to determine the shear strain, where the angle between the shear zone and foliation trace varies about 40° near the margin and gradually decreases to about 5° at the centre of shear zone. It is known<sup>3</sup> that

$$\text{Shear strain } (\gamma) = 2/\tan 2\theta.$$

Thus in the area the shear strain ( $\gamma$ ) at the centre of the shear zone reaches up to 12.56 and it gradually decreases up to 1.86 towards the shear zone boundary.

Strain within the shear zone has been computed from thin sections prepared parallel to the *XZ* plane (marked by rectangle in Figure 3 *d*) of the gneissic rock of the area. The shape and orientation of quartz grain, across a ductile shear zone, reflects that the strain is higher in the centre of the shear zone and it progressively decreases towards the shear zone boundary<sup>9</sup>. The preferred orientation of quartz *c*-axes across the shear zone<sup>9</sup> (Figure 3 *d*) reveals that close to the shear zone boundary (Figure 4 *a*), the quartz *c*-axes exhibit a weak girdle which is oblique to foliation and normal to the shear zone boundary, whereas in the centre of the shear zone (Figure 4 *c*), it exhibits a well-defined single girdle with *c*-axes maxima normal to foliation and shear zone boundary (Figure 4). Thus, the single girdle pattern of quartz *c*-axes appears to have developed at the shear zone boundary and becomes prominent in the centre of the shear zone with an increase in magnitude of shear deformation. Similar single girdle patterns in quartz grains have been inferred to have developed by simple shear<sup>18</sup>. The asymmet-



ric pattern indicates a non-coaxial strain history, while the direction of asymmetry with respect to shape fabric reflects the sense of shear<sup>19</sup>.

The MCT zone of Bhagirathi valley exhibits millimetre to kilometre-scale ductile and brittle-ductile shear zones (Figure 3). Data on mesoscopic ductile and brittle-ductile shear zones were collected along road-cuttings and the river valley. A detailed map (Figure 2) of the area shows preferred orientation of sinistral and dextral shear zones. The strike of sinistral shear zones varies between NNE and ENE, while that of dextral shear zones varies between NNW and WNW directions. In some places, shear zones develop on flat surfaces and the third dimension is not visible/available for measurement. At such localities, only the strike direction could be measured. However, most of the shear zones dip steeply (Figure 5a); hence strike directions are more significant than the amount of dip. Therefore, in addition to the stereogram, the rose diagram for the strike of the shear zone has been prepared (Figure 5b, where preferred orientations are better highlighted). In many outcrops, sinistral and dextral shear zones form a conjugate pair (Figure 3a). Therefore, in some places sinistral shear zones and dextral shear zones are noted to offset each other. Early-formed shear zones may be displaced by a later formed zone with the same or opposite sense of displacement. During progressive deformation, this is the general relationship between simultaneously developing sinistral and dextral shear zones<sup>10,20</sup>. Therefore, the NE-striking sinistral shear zones and NW-striking dextral shear zones

are inferred as a conjugate pair developed during the same deformational episode. They are thus useful for determining the principal compression directions.

To study the variation in compression direction in the MCT zone of Bhagirathi Valley, the area has been divided into four homogeneous sub-areas (Figure 2). Poles to the shear planes were plotted on the lower hemisphere of equal area net and contoured (Figure 5a) for each sub-area. The plots (Figure 5a) suggest that these shear planes occur in a conjugate system of two sets (dextral and sinistral). From the stereoplots of different sub-areas, the mean strike of sinistral and dextral shear zones of different sub-areas of the Bhagirathi Valley, have been determined (Table 1). Both these sets have developed during the same deformational episode as conjugate sets, and hence have been used to determine compression direction.

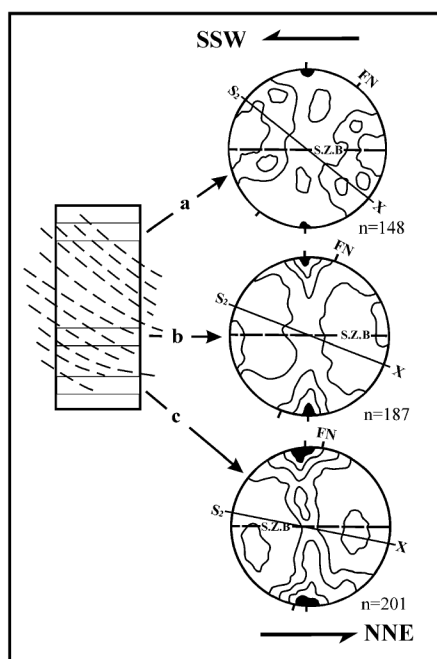


**Figure 4.** Quartz *c*-axes fabric from a ductile shear zone from shear zone boundary (a) to centre of shear zone (c). Contour intervals 2, 4, 6, >6% per unit area. Black shade represents highest contour value. S2: foliation plane; X: Lineation; SZB: Shear zone boundary; FN: Foliation normal.

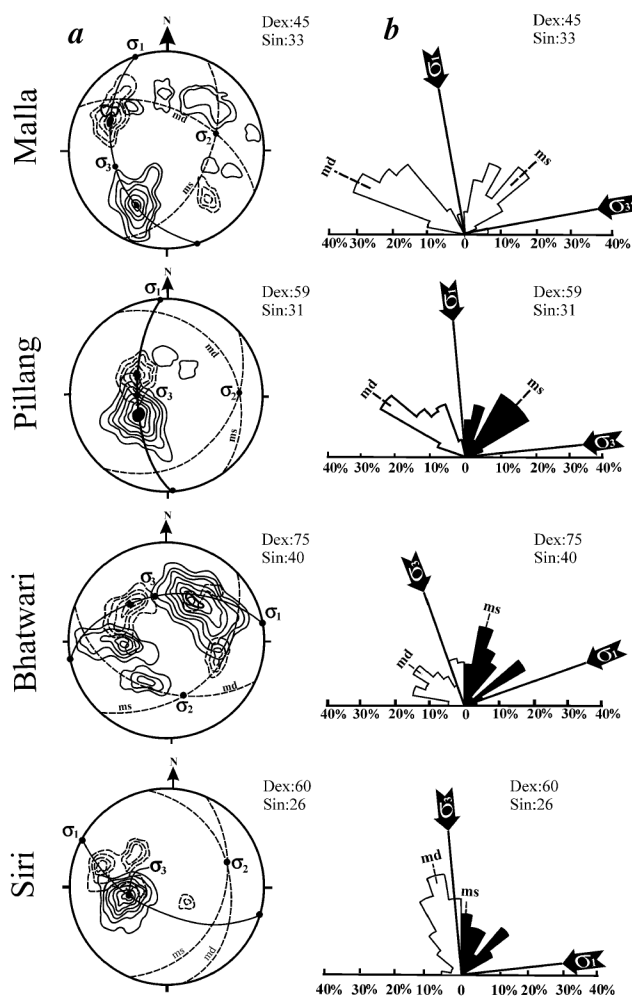


**Figure 5.** a, Synoptic orientation diagram of ductile and brittle-ductile shear zones from different sub-areas. Contour intervals 1, 2, 3, 4, 5, 6, >6% per unit area. Continuous contour lines represent dextral shear zones and dashed contour lines represent sinistral shear zones. b, Synoptic rose diagram of ductile and brittle-ductile shear zones from different sub-areas. ms, Mean sinistral; md, Mean dextral.  $\sigma_1$ ,  $\sigma_2$  and  $\sigma_3$  are maximum, intermediate and minimum compressive directions respectively.



**Table 1.** Modal orientation of shear zones and compression directions as determined from stereoplots

Sub-area	Mean strike of sinistral shear zone	Mean strike of dextral shear zone	$\sigma_1$	$\sigma_3$
Malla	N25°–N205°	N115°–N295°	0/N344°	44/N252°
Pillang	N40°–N220°	N145°–N325°	0/N358°	66/N269°
Bhatwari	N48°–N228°	N105°–N285°	0/N82°	50/N348°
Siri	N20°–N200°	N170°–N350°	0/N306°	58/N220°

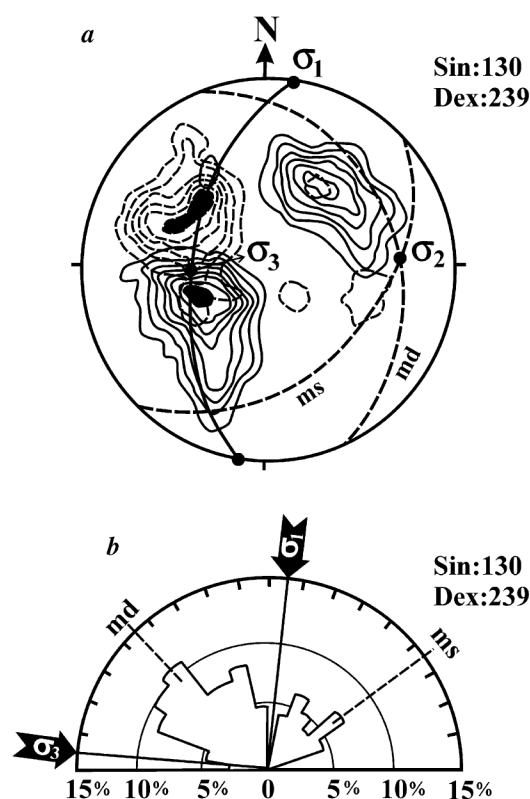


**Figure 6.** *a*, Synoptic orientation diagram of all the ductile and brittle-ductile shear zones from Bhagirathi Valley. Contour intervals 1, 2, 3, 4, 5, 6, >6%. Continuous contour lines represent dextral shear zones and dashed contour lines represent sinistral shear zones. *b*, Synoptic rose diagram of all ductile and brittle-ductile shear zones from Bhagirathi Valley. ms, Mean sinistral, md, Mean dextral.  $\sigma_1$ ,  $\sigma_2$  and  $\sigma_3$  are maximum, intermediate and minimum compressive directions respectively.

It is well known that in contrast to brittle deformation<sup>21</sup>, the obtuse bisector between the shear planes in ductile deformation parallels the maximum compressive direction ( $\sigma_1$ ). The minimum compression direction ( $\sigma_3$ ) is given by the acute bisector and the zone intersection parallels the intermediate compression direction ( $\sigma_2$ ). However, this geometry of stress axes is strictly correct at the time of initiation of shear zones<sup>17</sup>. Figure 5*a* suggests that the maximum compressive stress direction varies from sub-area to sub-area (near Malla 0/N344°; Pillang 0/N358°; Bhatwari 0/N82° and Siri 0/N306°) suggesting that  $\sigma_1$  varies from NNW to ENE direction

with horizontal compression. This variation of orientation in the compressive direction is probably due to the later phases of deformations.

Further, during progressive deformation, shear zones rotate with respect to each other and the stress field<sup>17</sup>. Also, because the shear zones are likely to be strain softened, there is probably quite a range of possible stress orientations that could activate them without initiating new ones<sup>17</sup>. Though the shear zones rotate during progressive deformation, the direction of bulk-shortening (obtuse bisector) and bulk-stretching (acute bisector) maintains nearly constant orientations<sup>20</sup>. Therefore, unless the shear field undergoes significant change, bisectors of preferred orientations of conjugate shear zones should give a reasonable measure of large-scale compression direction<sup>22</sup>. The results obtained from stereoplots (Figure 5*a*) were compared with those from the rose diagrams (Figure 5*b*) of strike of shear zones. In Figure 5*b*, strike directions of sinistral and dextral shear were plotted separately for all the four sub-areas of the Bhagirathi Valley, where preferred orientations are highlighted. From the bisectors of mean strike directions of shear zones of each rose diagram (Figure 5*b*), maximum and minimum compressive stress directions have been determined (Table 2).

In order to get the overall picture of stress directions in the Bhagirathi Valley, data collected from all the four sub-areas have been again plotted together on the stereonet (Figure 6*a*). This suggests a well-defined mean orientation. The sinistral shear zone strikes N48–N228 (mean value) and dextral shear zone strikes N 330–N150 (mean value). The bisector of these gives the orientation of  $\sigma_1$ ,  $\sigma_2$  and  $\sigma_3$ , which is 0/N10°, 28/N86° and 56/N268° respectively (Figure 6*a*). Similarly, the synoptic rose diagrams (Figure 6*b*) also reveal that  $\sigma_1$  trends N05° and  $\sigma_3$  N95°. Thus, both the plots (Figure 6*a* and *b*) suggest that the mesoscopic ductile shear zones in the MCT zone of Bhagirathi Valley were formed in response to nearly NNE–SSW horizontal compression. The concentration of datapoints in Figure 5*a* (Bhatwari and Malla sub-areas) and in Figure 6*a* are distributed mainly in the northeastern and southwestern quadrants. This may be attributed to the rotation of moderately to steeply dipping shear planes during later phases of deformation.

The deformation history of the area reveals that the rocks of the MCT zone of Bhagirathi Valley have suffered three phases of deformation, *D1*, *D2* and *D3*. According to Metcalfe<sup>11</sup>, the earliest *D1* deformation is represented by coaxial strain with no evidence of any rotational component. *D2*



deformation is represented by non-coaxial strain initiated during movement along the MCT zone. The main penetrative shear fabric found throughout the MCT zone is assigned to the *D2* deformation and numerous kinematic indicators showing NNE–SSW-directed sense of shear testify to the non-coaxial nature of this event<sup>11</sup>. Thus, *D2* deformation is responsible for synchronous development of mesoscopic ductile shear zones and translation of the MCT (Figure 7). The stretching lineation in the MCT zone trend towards northern direction (Figure 2) is regarded to be parallel to the thrust transport direction, which is normal to the Himalayan belt<sup>18</sup>. *D3* deformation is mainly responsible for the brittle deformation.

The strain studies reveal that the mesoscopic ductile shear zones developed in response to a high strain in a narrow zone, which even deforms the internal fabrics of the rocks. The quartz *c*-axis fabrics in mesoscopic shear zones demonstrate that the single girdle pattern of quartz *c*-axis appears to have developed at the shear zone boundary and becomes prominent at the centre of the shear zone with increase in shear strain.

The mesoscopic shear zones exhibit variation in strike from NNE to ENE and NNW to WNW directions. They are steeply dipping sinistral and dextral shear zones that formed as a conjugate pair and developed during the ductile shearing deformation, when S–C fabrics and other mylonitic structures developed. The two sets of shear zones developing simultaneously with opposing sense of movement would tend to lock each other. Otherwise a void would be created<sup>17</sup>. The obtuse bisectors of these conjugate shear

zones (sinistral and dextral) give nearly NNE–SSW horizontal compression. The differential movement of the MCT sheet is reflected in the random orientation of maximum compressional direction and can be correlated to the northward crustal movement of the Indian Plate below the Tibetan Plate. Thus, the mesoscopic ductile shear zones of Bhagirathi Valley, Garhwal Himalaya are developed in response to nearly NNE–SSW maximum horizontal compression, synchronous to the translation of MCT, which took place during the northward movement of the Indian Plate<sup>11</sup>.

**Table 2.** Modal orientation of shear zones and compression directions as determined from Rose diagram

Sub-area	Mean strike of sinistral shear zone	Mean strike of dextral shear zone	$\sigma_1$	$\sigma_3$
Malla	N45–N225	N295–N115	N350	N80
Pillang	N45–N225	N305–N125	N355	N85
Bhatwari	N15–N195	N305–N125	N70	N340
Siri	N05–N185	N345–N165	N85	N355

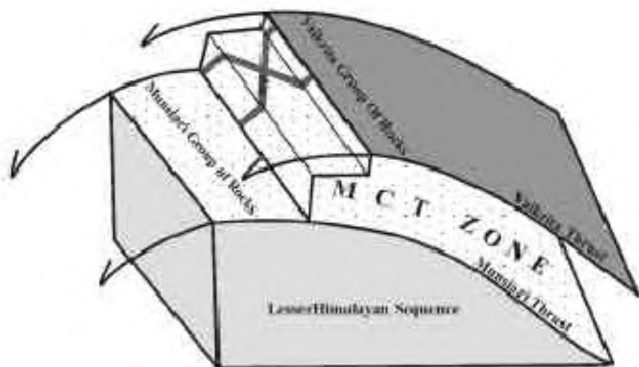


**Figure 7.** Schematic diagram showing translation of MCT over rocks of lesser Himalayan sequence Munsiri Thrust and Vaikrita Thrust-bound MCT zone, in which conjugate ductile shear zones are developed.

1. Choukroune, P. and Gapais, D., Strain pattern in the Aar granite (Central Alps): Orthogneiss developed by bulk inhomogeneous flattening. *J. Struct. Geol.*, 1983, **5**, 411–418.
2. Ramsay, J. G. and Allison, I., Structural analysis of shear zones in an alpinised Hercynian granite, Maggia Nappe, Pennine Zone, Central Alps. *Schweiz. Miner. Petrogr. Mitt.*, 1979, **59**, 251–279.
3. Ramsay, J. G. and Graham, R. H., Strain variations in shear belts. *Can. J. Earth Sci.*, 1970, **7**, 786–813.
4. Hara, I., Takeda, K. and Kimura, T., Preferred lattice orientation of quartz in shear deformation. *Hiroshima Univ. J. Sci. C*, 1973, **7**, 1–10.
5. Coward, M. P., Flat lying structure within the Lewisian basement gneiss complex of NW Scotland. *Proc. Geol. Assoc.*, 1974, **85**, 459–472.
6. Srivastava, H. B., Hudleston, P. J. and Early, D., Strain and possible volume loss in a high-grade ductile shear zone. *J. Struct. Geol.*, 1995, **17**, 1217–1231.
7. Hudleston, P. J., Progressive deformation and development of fabric across zone of shear in glacial ice. In *Energetics of Geological Processes* (eds Saxena, S. and Bhattacharji, S.), Springer Verlag, New York, 1977, pp. 121–187.
8. Simpson, C., Determination of movement sense in mylonites. *J. Geol. Educ.*, 1986, **34**, 246–261.
9. Srivastava, H. B., Sahai Atul and Lal, S. N., Strain and crystallographic fabrics in mesoscopic ductile shear zones of Garhwal Himalaya. *Gondwana Res.*, 2000, **3**, 395–404.
10. Ramsay, J. G., Shear zone geometry: A review. *J. Struct. Geol.*, 1980, **2**, 83–93.
11. Metcalfe, R. P., Pressure, temperature and time constraints on metamorphism across the Main Central Thrust zone and High Himalayan Slab in the Garhwal Himalaya. In *Himalayan Tectonics* (eds Trelor, P. G. and Searle, M. P.), Geol. Soc. Spl. Publ., 1993, vol. 74, pp. 485–509.
12. Valdiya, K. S., The two intracrustal boundary thrusts of Himalaya. *Tectonophysics*, 1980, **323**, 323–348.
13. Heim, A. and Gansser, A., Central Himalaya: Geological observation of the Swiss Expedition in 1936. *Mem. Soc. Helv. Sci. Nat.*, 1939, **73**, 1–245.
14. Jain, A. K., Stratigraphy and tectonics of Lesser Himalayan region of Uttarkashi Garhwal Himalaya. *Himalayan Geol.*, 1971, **1**, 25–57.
15. Singh, K. and Thakur, V. C., Microstructure and strain variation across the footwall of the Main Central Thrust Zone, Garhwal Himalaya. *J. Asian Earth Sci.*, 2001 **19**, 17–29.
16. Berthe, D., Choukroune, P. and Jegouzo, P., Orthogneiss mylonite and coaxial deformation of granites: The example of the South American shear zone. *J. Struct. Geol.*, 1979, **1**, 31–42.
17. Mukhopadhyay, D. K. and Haimanot, B. W., Geometrical analysis and significance of mesoscopic shear zones in the Precambrian gneisses around Kolar Schist belt, South India. *J. Struct. Geol.*, 1989, **11**, 569–581.
18. Bouchez, J. L. and Pecher, A., The Himalayan Main Central Thrust Pile and its quartz rich tectonites in Central Nepal. *Tectonophysics*, 1981, **78**, 23–50.



19. Price, G. P., Preferred orientations in quartzites. In *Preferred Orientation in Deformed Metals and Rocks: An Introduction to Modern Texture Analysis* (ed. Wenk, H. R.), Academic Press, New York, 1985, pp. 385–406.
20. Ramsay, J. G. and Huber, M. I., *The Techniques of Modern Structural Geology, Folds and Fractures*. Academic Press, New York, 1987, vol. 2.
21. Park, R. G., Shear zone deformation and bulk strain in granite–greenstone terrain of the Western Superior Province, Canada. *Pre-cambrian. Res.*, 1981, **14**, 31–47.
22. Anderson, E. M., *The Dynamics of Faulting*, Oliver and Boyd Edinburgh, 1951.

ACKNOWLEDGEMENTS. The research was supported by Department of Science and Technology, New Delhi.

Received 16 July 2004; revised accepted 6 November 2004

## Reliable natural recharge estimates in granitic terrain

Ramesh Chand\*, G. K. Hodlur, M. Ravi Prakash, N. C. Mondal and V. S. Singh

National Geophysical Research Institute, Uppal Road, Hyderabad 500 007, India

**The average natural recharge to the aquifer of Kongal river basin located in Nalgonda district, Andhra Pradesh, India due to the monsoons is estimated using injected tritium technique at a few selected sites. Kriging and Thiessen Polygon methods are employed to interpolate recharge estimates and arrive at more realistic values. The estimate is made from the spatial distribution of recharge values. The spatial distribution of recharge values is derived from 25 site-specific measurements. The quantum of groundwater recharge through vertical infiltration has been estimated as 27.5 and 30.0 mm ( $I^{-2}$ ) by Kriging and Thiessen polygon methods respectively; a value of 25.0 mm ( $I^{-2}$ ) was arrived at using average recharge values in the area. The total rainfall during the corresponding period is 566.67 mm ( $I^{-2}$ ) and thus the fractional amount of recharge is 5% of the rainfall.**

GROUNDWATER abstraction has increased to complement the increasing water demand by the continuously growing population. Groundwater recharge to the aquifer system is thus the most important variable to be estimated. Its estimation is thus an important input for a rational exploitation and management of groundwater resources. A reliable estimation of recharge in hard-rock aquifers is a difficult task in view of wide spatial–temporal variations in the hydrological and hydrometrological conditions. It may be estimated by several conventional methods such as groundwater

balance, lysimeter, etc. These methods require analysis of large volumes of hydrological data (precipitation, surface run-off, evapo-transpiration, change in groundwater storage, etc.) accumulated over a considerable time span, which is generally inadequate, lacking or unreliable in many areas<sup>1–3</sup>. The tracer technique is a direct method for estimation of groundwater recharge<sup>4–6</sup> at the site-specific point. Extensive research has been done in the allied fields during the last four decades<sup>7–16</sup>. Here an attempt has been made to estimate recharge in the area by the injected tritium technique and to also estimate the spatial variation of recharge by Kriging and Thiessen methods.

Integrated hydrogeological and geophysical studies were carried out by National Geophysical Research Institute (NGRI), Hyderabad in the Kongal river basin, located in Nalgonda district, Andhra Pradesh, India (Figure 1a). The aim was to develop an appropriate methodology for groundwater management and development. Estimation of natural recharge from precipitation was an important component of this work. Natural recharge to the shallow aquifer takes place through the movement of percolated rain water through the vadose zone, till it reaches the water table. Hence it depends upon many parameters, namely porosity, permeability, infiltration capacity of the soil, amount of rainfall, and its variation in space and time domains. Recharge estimates are arrived at by averaging the recharge values estimated at a few representative sites in the region. Hence, in any given area, if the number of data points gives the recharge values at the representative sites, the accuracy level of the recharge estimate of the area improves and tends to become a more realistic evaluation of the parameters. An attempt has been made to utilize the Krige estimates to obtain recharge values for the sites, using neighbouring field-estimated values falling with a certain distance. Using such statistically generated large values, the total recharge of the study area has been arrived at.

The study area is about 50 km east of Hyderabad. It covers an area of 180 km<sup>2</sup> of the Kongal river (Figure 1a) and lies between 78°48'38"–79°03'25"E long. and 17°07'48"–17°16'48"N lat. Most of the area is covered by pink granite. The area is devoid of major strike like folds and faults. Joint patterns are not common in exposures. Many basic dykes, which are fine-grained dolerite, traverse the granite. These dykes are spread throughout the basin. These are NS, NW–SE, NE–SW and EW trending dykes. A small strip of kankar, which is silty and clayey, is exposed in the southwestern zone and also the northeastern part. The area is drained by Kongal river, and its main network of streams is shown in Figure 1a. The river flows NW to SE and passes through Palwela village. Surface water bodies such as lakes are spread out in the southeastern part of the basin. The area is in general a flat terrain without major topographical relief like hills and valleys. The drainage of the area clearly indicates the slope of the terrain, which is NW to SE. Groundwater occurs in shallow-weathered and deep-fractured granite in the western and northwestern parts, whereas in the remaining area it occurs in weathered gneisses. The depth to water level

\*For correspondence. (e-mail: rameshtyagi@yahoo.com)